ISSN 1075-7015, Geology of Ore Deposits, 2015, Vol. 57, No. 6, pp. 522–535. © Pleiades Publishing, Ltd., 2015.

Phase Separation of Ore Forming Fluid Related to Gold Mineralization in Wynad Gold Field, Southern Granulite Terrain, India: Evidences from Fluid Inclusion Studies[1]

Ajit Kumar Sahoo[a], R. Krishnamurthi[a], and Saju Varghese[b]

[a]*Department of Earth Sciences, Indian Institute of Technology Roorkee, Uttarakhand-247 667, India*

[b]*Geological Survey of India, DK Block, GSI Complex Karunamoyee, Salt Lake, Kolkata-700091, India*

e-mail: krishnamurthi.iitr@gmail.com

Received June 28, 2014

Abstract—Fluid inclusion studies were carried out on auriferous quartz veins of Wynad Gold Field, Southern Granulite Terrain of India. Three types of primary fluid inclusions have been observed; Type-I: H_2O–CO_2 inclusions, Type-II: CO_2 inclusions and Type-III: aqueous inclusions. The Type-I and Type-II inclusions are more abundant than Type-III inclusions. The coexistence of Type-I and Type-II inclusions are common within quartz grains in most of the samples studied. Variation in phase ratio and broad range of total homogenization temperature of Type-I and Type-III inclusions (i.e. 194°C to 300°C and 189°C to 282°C, respectively) indicate the entrapment of heterogeneous fluid in inclusions. This heterogeneity could be due to phase separation of original low saline H_2O–CO_2 ore fluid in response to drop in pressure and temperature. Gold along with other constituents could have precipitated in response to phase separation of the ore fluid.

DOI: 10.1134/S107570151506001X

INTRODUCTION

Hydrothermal solutions (fluids) generally consist of water with volatiles (CO_2, CH_4, N_2, sulfur species and so on), dissolved components of metals and salts at elevated temperature and pressure. These hydrothermal solutions have been considered to produce huge metal deposits of Cu, Pb, Zn, Au, Ag and so on in different geological setting. Such solutions with different components might have come from either a single or multiple sources such as magma, mantle, rocks, meteoric water and sea water (Misra, 2000). Being less dense, they find suitable ways or make their own ways to come up. During upwelling they are subjected to changes in physicochemical conditions that will lead to deposition of the dissolved metals present in the fluids.

Lode gold deposits that are often categorized as orogenic gold deposits and characterized by: i—gold-quartz (± calcite) veins hosted in metamorphic rocks irrespective of grade of metamorphism and age, ii—spatial association with convergent tectonic set-up, iii—high enrichment of some of the rare metals like Au, Ag, As, W, Sb, B, Bi, Pd and Te with very low enrichments of Cu, Pb and Zn, and iv—hydrothermal alterations involving massive introduction of CO_2, K, S and H_2O (Fyfe and Kerrich, 1982; Groves, 1993; Christopher and Vanderhor, 1998; Zhang et al., 2012). Fluid inclusion studies of this type of gold deposits indicate that the hydrothermal fluids involved in mineralization are: 1—low to moderately high temperature (200–500°C), 2—H_2O–$CO_2 \pm CH_4$ rich, 3—low to moderate saline and 4—near-neutral to alkaline pH (Groves et al., 1998; Ho et al., 1985; Mikucki, 1998; Ridley et al., 1996). Experimental and thermodynamic calculations indicate that gold is generally dissolved in hydrothermal solutions as sulfide and chloride complexes (Benning and Seward, 1996; Seward, 1973; Seward, 1984). Sulfide complexes are thought to be the major dissolved form of transport of gold in case of lode gold deposits (Groves et al., 1998; Mikucki, 1998). The reasons for the deposition of gold from high temperature fluids are change in P-T conditions, phase separation, wall rock alteration and surface chemistry-driven processes (Mikucki, 1998; Williams-Jones et al., 2009). The phase separation is one of the noteworthy processes for the deposition of gold in significant amount. This mechanism has been proposed based on the fluid inclusion studies (Caulibaly et al., 2008; Zhang et al., 2012).

The Wynad Gold Field (WGF) of Southern Granulite Terrain (SGT), India, is known for ancient mining activity for gold (Radhakrishna and Curtis, 1999) and the mining activity in this region dates back to 1875 (King, 1878). Several old workings along with high grade gold bearing quartz reefs (10–11 g/t of Au) were discovered by British geologists in the nineteenth century. In WGF, gold has been reported as: 1—primary gold associated with quartz and sulfide minerals within quartz veins and 2—secondary gold associated with laterite and placer (Binu Lal et al., 2003; Krish-

[1] The article is published in the original.

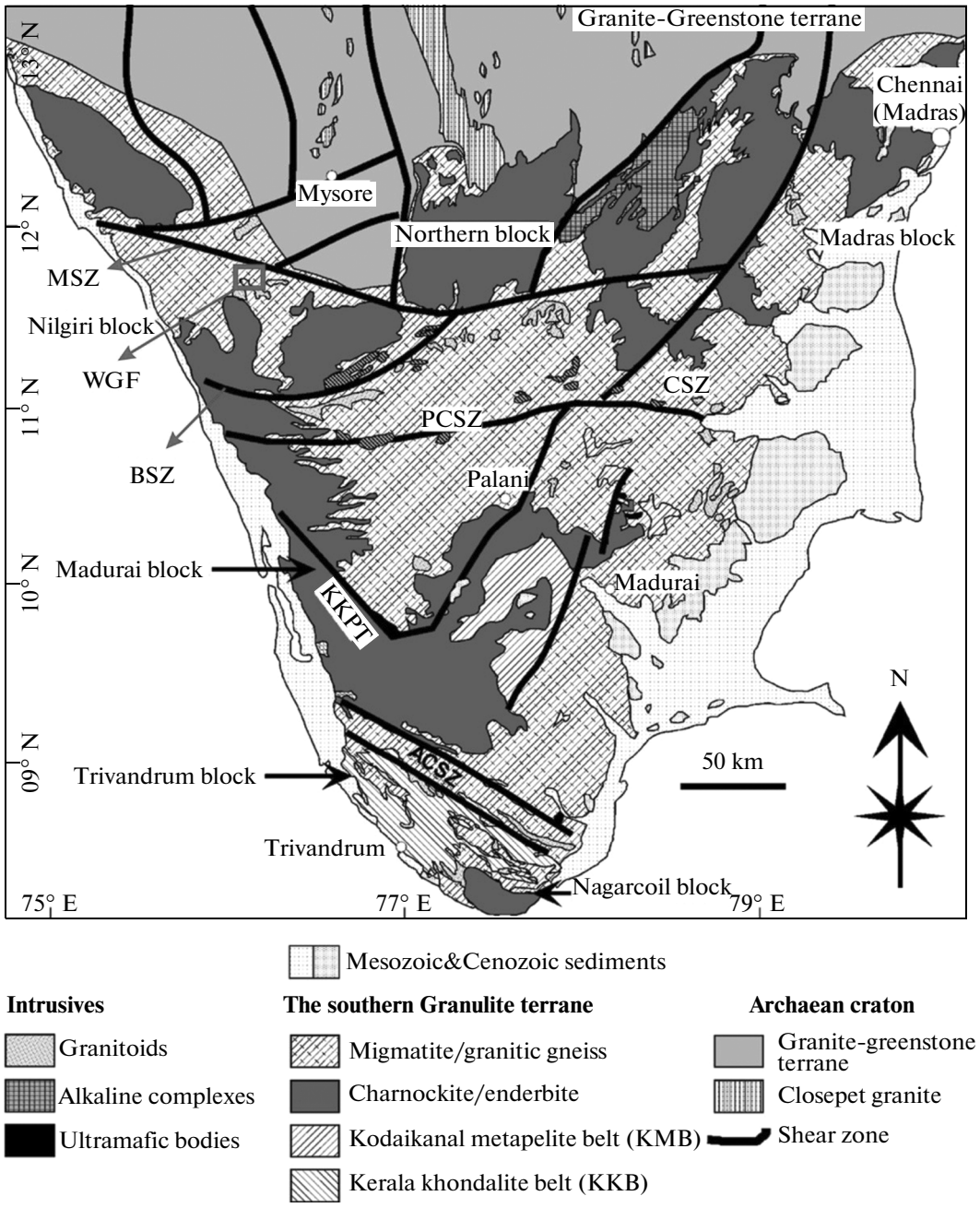

Fig. 1. Geological map of the Southern Granulite Terrain (Santosh and Sajeev, 2006). WGF—Wynad Gold Field; MSZ—Moyar Shear Zone; BSZ—Bhavani Shear Zone; PCSZ—Palghat Cauvery Shear Zone; CSZ—Cauvery Shear Zone; KKPT—Karur-Kambam-Painavu-Trichur shear zone; ACSZ—Achankovil Shear Zone.

namurthi, 2013). The deposition of primary gold within quartz veins was attributed to phase separation of original immiscible H_2O–CO_2 fluid (Binu Lal et al., 2003). But, concrete evidences for the phase separation mechanism were not given by Binu Lal et al. (2003). In this paper, we present certain new evidences such as presence of primary CO_2 fluid inclusions and coexistence of H_2O–CO_2 inclusions with CO_2 inclusions in auriferous quartz veins of WGF. Petrographic and microthermometric record of the inclusions related to gold-sulfide-quartz veins of the WGF indicating phase separation of the ore fluid leading to deposition of gold has been discussed in this paper.

REGIONAL GEOLOGY

The SGT is one of the Proterozoic orogens in southern Peninsular India, comprising high grade metamorphic rocks like charnokite, khondalite and migmatite invaded by younger pegmatite intrusives (Fig. 1; Chetty and Santosh, 2013; Soman, 2002). It is a collage of crustal blocks which are separated by the

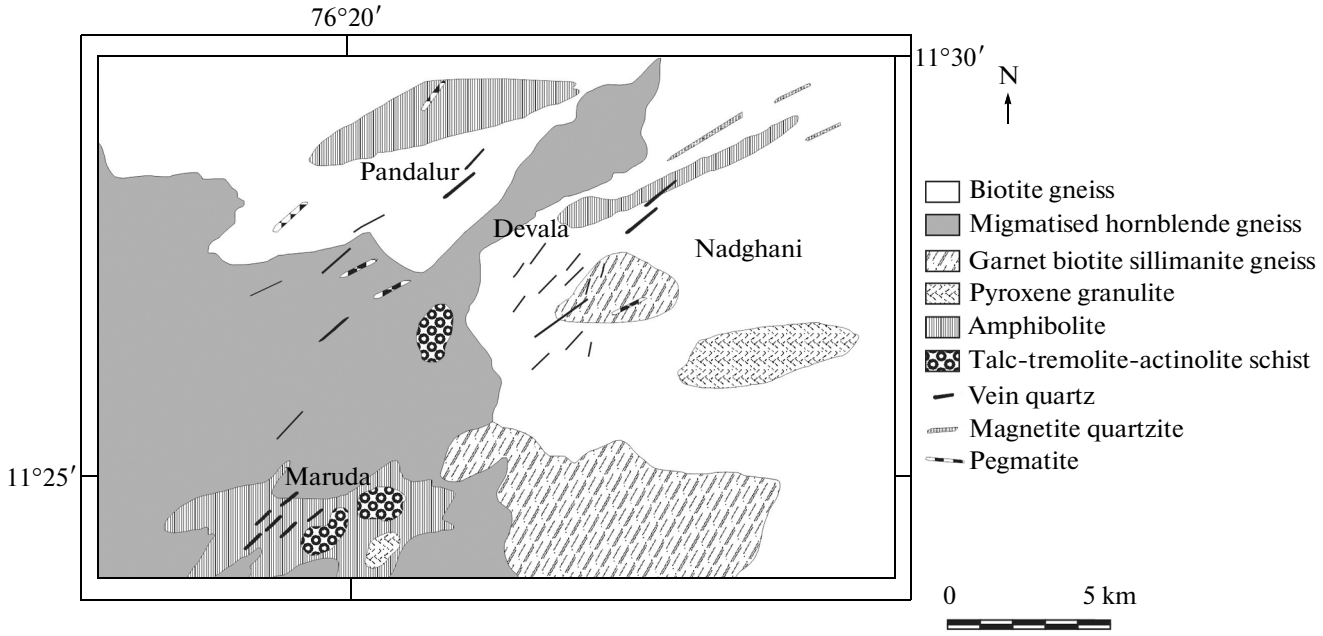

Fig. 2. Geological map of the Wynad Gold Field (after Binu-Lal et al., 2003).

Cauvery Shear Zone (CSZ) and the Achankovil Shear Zone (ACSZ) (Chetty and Santosh, 2013; Chetty et al., 2006). The CSZ marks the boundary of two major crustal blocks of SGT namely the Archean granulite block to the north and the Neoproterozoic granulite block to the south (Chetty and Santosh, 2013).

The CSZ trends E–W and consists of a set of parallel pervasive shear zones. The Moyar Shear Zone (MSZ), which hosts the mineralized quartz veins of WGF, is the northern most shear zone of CSZ (see Fig. 4 of Chetty and Santosh, 2013). The MSZ runs about 200 km from west to east and merges with Bhavani Shear Zone (BSZ) at the eastern periphery of the Nilgiri Block. The shallow to steeply plunging stretching lineations characterize these shear zones of CSZ (Chetty and Santosh, 2013). Such multi-scale structural observations along the CSZ are suggestive of typical transpressional tectonics (Chetty and Rao, 1998). The CSZ has undergone two major phases of deformation. The first phase of deformation took place in the Neoarchean period and the second one in the Neoproterozoic period (Chetty and Santosh, 2013; Santosh et al., 2012).

LOCAL GEOLOGY AND MINERALIZATION

WGF is located immediately south of the MSZ (Fig. 1). The area comprises mainly migmatitised hornblende gneiss, amphibolite, biotite gneiss, garnet-biotite-sillimanite gneiss, pyroxene granulite, magnetite quartzite and talc-tremolite-actinolite schist (Binu Lal et al., 2003; Pruseth et al., 2011). The auriferous hydrothermal quartz veins are hosted in amphibolite and gneisses (Fig. 2). The veins generally strike along NE-SW direction and cut the regional trend of foliation. The discordant relationship of the auriferous quartz veins with respect to foliation of host rocks and age of emplacement of mineralized quartz veins (~450 Ma) determined by Pruseth et al. (2011) suggest that the veins were formed after the Neoproterozoic tectonothermal event. Chloritization, sericitization, sulfidation and carbonatization represent the hydrothermal alteration of the host rocks in the area (Binu Lal et al., 2003; Pruseth et al., 2011). In the auriferous quartz veins, the dominant sulfide minerals are pyrite, pyrrhotite, arsenopyrite and chalcopyrite. Visible gold grains have been reported as native gold, inclusions in pyrite and, as micro-veinlets within pyrite and chalcopyrite (Binu Lal et al., 2003).

MATERIALS AND METHODS

Auriferous quartz vein samples were collected from WGF (around Devala, Maruda and Pandalur area; see Fig. 2) and twenty doubly polished wafers were prepared at Wadia Institute of Himalayan Geology, Dehradun. A Nikon ECLIPSE E200 petrological microscope was used for petrography of fluid inclusions and microthermometry was carried out using a Linkam THMSG 600 heating-freezing stage equipped on a Nikon LV 100 Pol microscope at the Department of Earth Sciences, Indian Institute of Technology, Roorkee. The unit operates in the temperature range of –196°C to + 600°C. The stage was periodically cal-

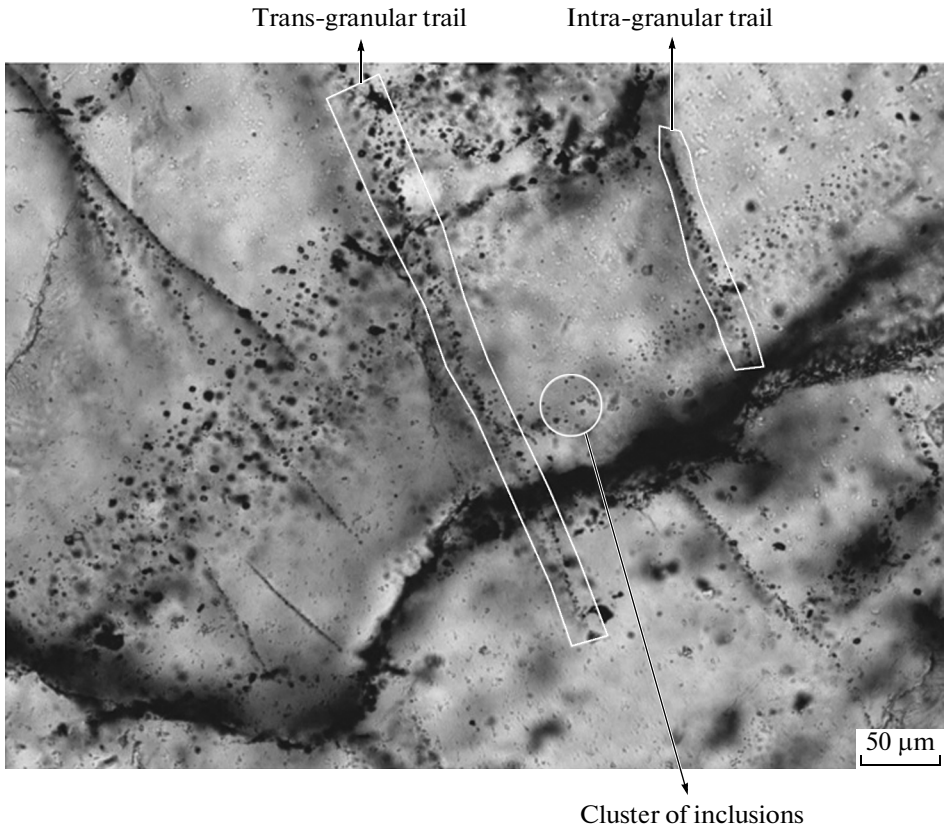

Fig. 3. Photomicrograph showing the distribution pattern of fluid inclusions.

ibrated by synthetic pure CO_2 inclusions (triple point = −56.6°C) in quartz. The samples containing suitable fluid inclusions were observed before the microthermometry. Salinity and density of fluids in inclusions were calculated by FLINCOR software (Brown, 1989) using appropriate equations.

RESULTS

Fluid Inclusion Petrography

In the samples of WGF, abundant inclusions were observed in doubly polished wafers prepared from mineralized vein quartz. The inclusions occur as clusters, along intra-granular trails as well as trans-granular trails and as isolated occurrence (Fig. 3). Criteria given by Roedder (1984) and Shepherd et al. (1985) were followed to distinguish primary, secondary and pseudo-secondary inclusions. The isolated inclusions and inclusions in clusters were considered as primary with respect to the formation of quartz vein. The inclusions in intra-granular trails and trans-granular trails were designated as pseudo-secondary and secondary, respectively. Only the primary inclusions (5–15 μm) were studied in detail. At room temperature two types of primary inclusions were observed, biphase liquid-vapour and monophase liquid inclusions (Fig. 4b). The inclusions were further classified based on microthermometry as Type-I: H_2O–CO_2 inclusions, Type-II: CO_2 inclusions and Type-III: aqueous inclusions (Fig. 5). The coexistence of Type-I and Type-II inclusions is very common (Fig. 4).

Type-I: H_2O–CO_2 inclusions. At room temperature these inclusions consist of two phases with a bubble in aqueous phase (Fig. 5a i), but during freezing a new phase appears exhibiting liquid H_2O, liquid CO_2 and vapour CO_2 (Fig. 5a ii). These inclusions range in size from 3 to 15 μm having different shapes such as rounded, tubular and irregular. The phase proportion (H_2O : CO_2) within such inclusions varies from 90 : 10 to 10 : 90 (table). These are the most abundant variety of primary inclusions observed in the doubly polished wafers.

Type-II: CO_2 inclusions. At room temperature these inclusions appear to be monophase (Fig. 5b i), but vapour phase appears during freezing (Fig. 5b ii). These inclusions homogenise to a single phase below room temperature during heating runs. The size of the inclusions ranges from 2 to10 μm having different shapes such as rounded, tubular, elongated and irregular. This type of inclusions are as abundant as Type-I inclusions.

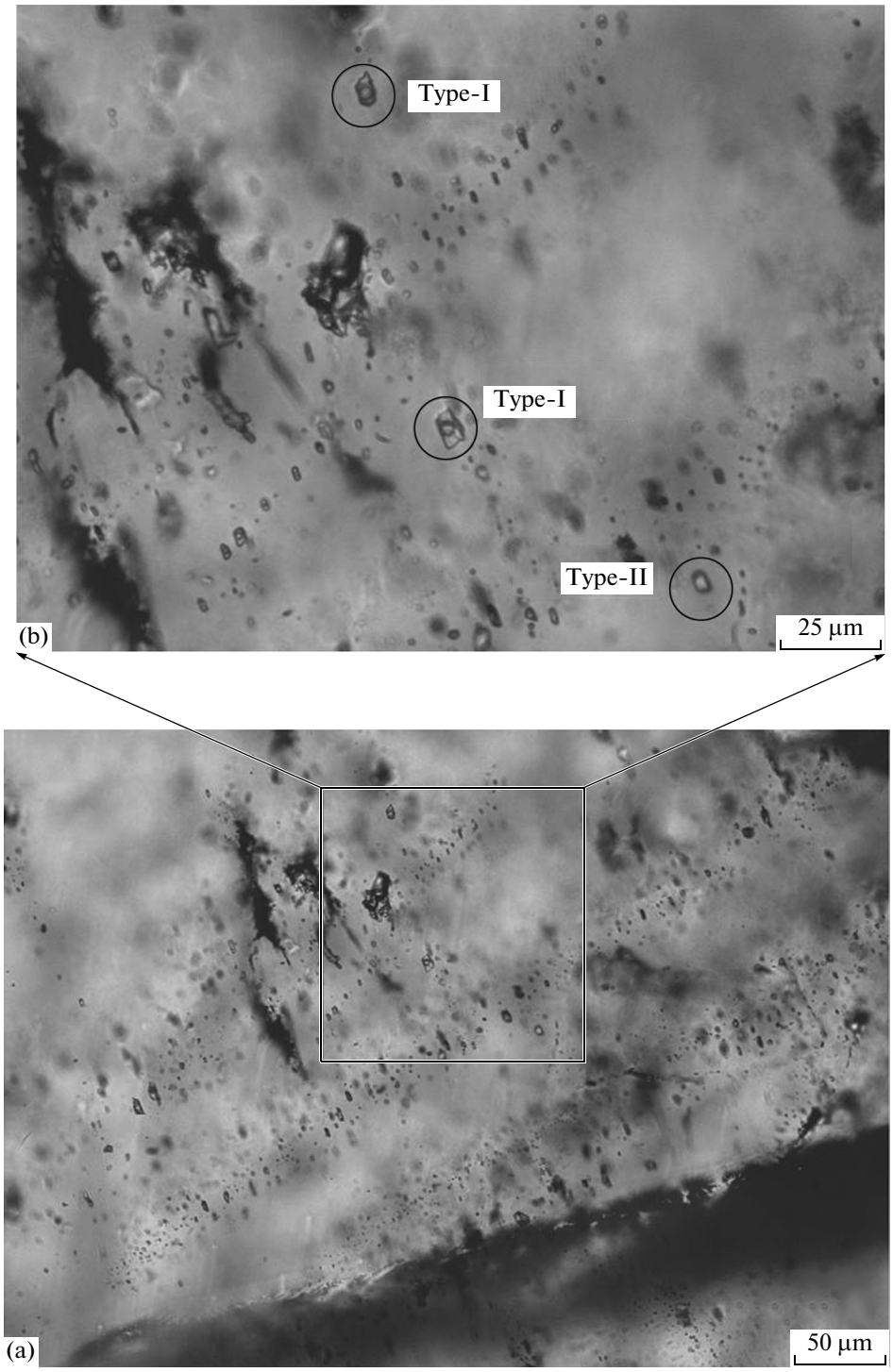

Fig. 4. Photomicrographs showing the co-existance of Type-I and Type-II inclusions (a) in plane polarized light and (b) magnified part of inset shown in (a).

Type-III: aqueous inclusions. At room temperature these inclusions appear as biphase with liquid H_2O and H_2O vapour (Fig. 5c i). Size of these inclusions range from 4 to12 μm with different shapes such as oblate and spherical. The liquid to vapour ratio in these inclusions range from 80 : 20 to 50 : 50 (table).

Microthermometry

Freezing data. The melting of CO_2 (T_m CO_2) in Type-I and Type-II inclusions occurred between −55.5°C and −60°C (Fig. 6a; table). In most of the inclusions the values of T_m CO_2 fall in the range of −56 to −57°C indicating the presence of pure CO_2. However, a few

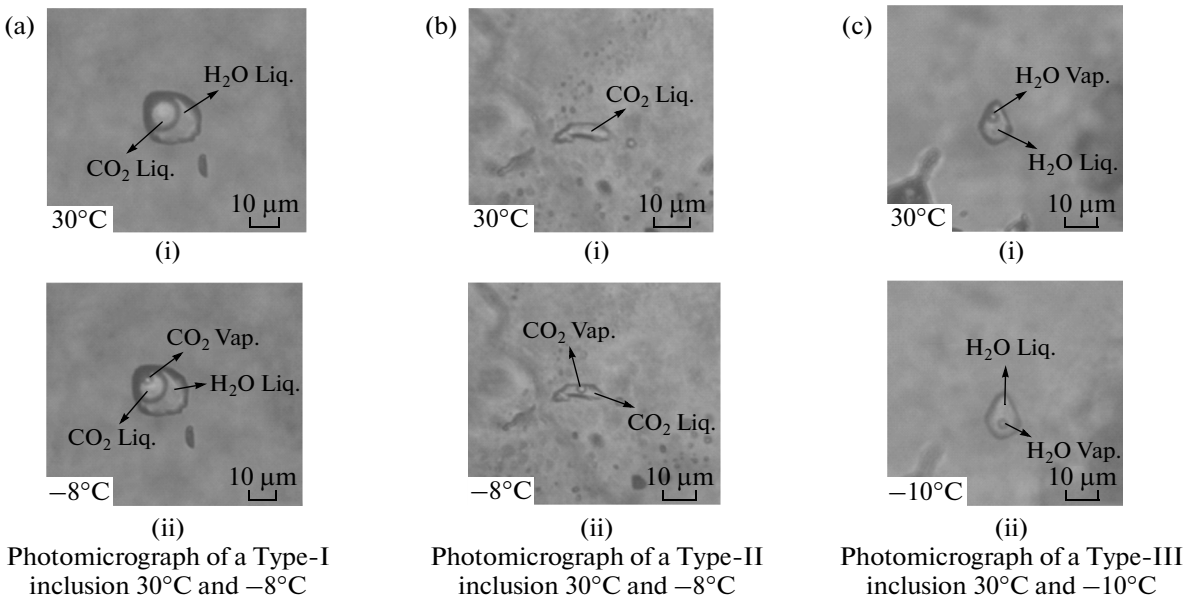

Fig. 5. Photomicrographs of Type-I, Type-II and Type-III primary fluid inclusions at different temperature.

inclusions show T_m CO_2 values around −60°C, which can be due to the presence of other gases like CH_4 and N_2 (Shepherd et al., 1985). The first melting of ice (T_{FM} ice) in most of the Type-I and Type-III inclusions occurred between −18°C to −29°C (table). But, in some inclusions it occurred between −37°C to −40°C (Fig. 6b). This data indicates the presence of different types of salts such as NaCl, KCl and $MgCl_2$ based on the eutectic temperature given in Shepherd et al. (1985). Final melting of ice (T_m Ice) in Type-III inclusions was observed in a temperature range from −1°C to −5°C (table) suggesting the salinities from 2 to 8 wt % NaCl equivalents (Fig. 6c, e). Melting of clathrate was observed in few larger Type-I inclusions. The temperatures of clathrate melting (T_m CL) are between 2°C and 8°C (Fig. 6d). Salinities deduced from the clathrate melting temperature are from 4 to 14 wt% NaCl equivalents (Fig. 6e).

Heating data. The homogenization of CO_2 (Th CO_2) in Type-I and Type-II occurred into liquid phase at temperature range of 4.7°C to 28.3°C and from −4°C to 28.3°C, respectively (Fig. 7a). Density of CO_2 present in the inclusions estimated by Th CO_2 values ranges from 0.64 to 0.95 (Fig.7b). The total homogenization of Type-I inclusions took place into both liquid and vapour phase at the temperature (Th TOT) range 194°C to 300°C (Fig. 8a; table). The Type-III inclusions homogenized into liquid phase at temperature range from 189°C to 282°C (Fig. 8b; table).

DISCUSSION

The auriferous quartz veins of WGF are hosted in the shear induced fractures of MSZ (Krishnamurthi, 2013). The age of emplacement of the auriferous quartz veins is about 450 Ma (Pruseth et al., 2011). This geo-chronological information indicates a possible temporal linkage between the gold mineralization in WGF and the last phase of Neoproterozoic deformation (Pan-African) event in MSZ. Based on the results of the present work, the condition of entrapment of fluid inclusions and P-T conditions of fluid activity pertaining to gold mineralization have been discussed below.

Conditions of Fluid Entrapment

The cause of heterogeneity of an original homogeneous fluid is phase separation. A single generation of fluid inclusions trapped from a heterogeneous fluid due to phase separation would be of different types with different phase proportions and phases (Roedder, 1984; Diamond, 2003). Diamond (2003) illustrated the heterogeneous entrapment of a single fluid inclusion assemblage (FIA) trapped within a growing crystal from fluid experiencing phase separation (Fig. 9). Five inclusions (1 to 5 in Fig. 9) of a FIA would have different phase proportion at the time of trapping as shown in Fig. 9b. Upon cooling each inclusion of that assemblage behaves differently because of different bulk properties at the time of trapping. Hence, at room temperature all the five inclusions will have different

Microthermometry data of primary fluid inclusions Type-I primary fluid inclusions

S.No.	$H_2O : CO_2$ at room temperature	$T_m CO_2$ (°C)	$T_h CO_2$ (°C)	T_h TOT (°C)	T_{FM} Ice (°C)	T_m CL (°C)	Salinity Wt % NaCl eq.
1	60 : 40	−56.9	+27.1(L)	246(L)	*	+8	3.89
2	40 : 60	−56.8	+25(L)	273(V)		+6	7.37
3	50 : 50	−56.8	+14(L)	271(V)	−18	+2.3	12.81
4	10 : 90	−56.6	+9.5(L)	221(V)	−21	+7.1	5.50
5	10 : 90	−56.6	+16(L)	258(V)	−24	+7.4	4.97
6	50 : 50	−56.6	+14(L)	289(L)	−19	+2	13.19
7	60 : 40	−56.7	+10(L)	281(V)	−21	+6	7.37
8	10 : 90	−56.9	+6.5(L)	236(V)	*	+5	8.97
9	50 : 50	−57	+11.5(L)	253(V)	−18	+7.6	4.61
10	10 : 90	−56.6	+9.6(L)	256(V)	*	+6.5	6.54
11	50 : 50	−56.8	+8(L)	246(V)	*	+4.2	10.18
12	50 : 50	−56.8	+17.4(L)	295(V)	*	+5	8.97
13	60 : 40	−56	+25.6 (L)	270(L)	*	+3	11.88
14	80 : 20	−56.7	+27(L)	283(V)	−29	*	*
15	60 : 40	−56.9	+28.3(L)	268(V)	−29	+6.5	6.54
16	50 : 50	−56.8	+24(L)	244(V)	−25	+5	8.97
17	80 : 20	−56.8	+7(L)	237(V)	*	+5	8.97
18	90 : 10	−56.4	+12(L)	256(L)	*	+6	7.37
19	60 : 40	−56.6	+21(L)	265(L)	−27.6	+5	8.97
20	60 : 40	−56.6	+14(L)	293(L)	*	+4	10.47
21	50 : 50	−56.6	+4.7(L)	194(V)	*	+3	11.88
22	60 : 40	−57.4	+22.6 (L)	230(V)	−18	+6	7.37
23	60 : 40	−57.2	+19.8(L)	255(V)	−20.4	+5.4	8.34
24	70 : 30	−59	+23.4(L)	298(L)	*	+6.2	7.04
25	35 : 65	−57.1	+27(L)	260(V)	*	*	*
26	50 : 50	−55.9	+27.2(L)	207(L)	−27	*	*
27	50 : 50	−56	+27.9(L)	277(L)	−27	+4.8	9.28
28	50 : 50	−56	+28(L)	242(L)	−27	*	*
29	70 : 30	−56.8	+13(L)	290(L)	−28	*	*
30	70 : 30	−55.9	+9.8(L)	267(L)	*	*	*
31	20 : 80	−55.9	+11(L)	212(V)	*	+7.3	5.15
32	80 : 20	−55.7	+13(L)	208(L)	−23	*	*
33	60 : 40	−56.8	+21.8(L)	222(L)	−19	*	*
34	60 : 40	−56.6	+14.7(L)	267(L)	−24.6	*	*
35	40 : 60	−56.9	+13.1(L)	291(V)	−27	+5.9	7.54
36	80 : 20	−57	+25.6(L)	288(L)	*	*	*
37	50 : 50	−56.8	+6.4(L)	247(L)	*	+2.7	12.28
38	60 : 40	−57.4	+12.9(L)	283(L)	−22	+7.9	4.07
39	50 : 50	−56.8	+14.8(L)	276(V)	*	+5	8.97
40	70 : 30	−56.6	+17(L)	256(V)	−27	*	*
41	90 : 10	−56.6	+22.8(L)	247(L)	−29	+3	11.88
42	60 : 40	−56.8	+17.6(L)	255(L)	*	+6.1	7.21
43	60 : 40	−56.6	+12(L)	262(L)	−24	+7	5.68
44	30 : 70	−57.1	+13.2(L)	208(V)	−26	+2.5	12.55
45	50 : 50	−56.7	+21(L)	218(L)	−21	+4.9	9.12
46	20 : 80	−57.3	+14.8(L)	252(V)	−28	*	*
47	60 : 40	−57.1	+12.5(L)	205(L)	*	+7	5.68
48	70 : 30	−56.6	+9.7(L)	217(L)	−29	*	*
49	30 : 70	−56.8	+11.6(L)	269(V)	−22	*	*

Type-II primary fluid inclusions

S.No.	$T_m CO_2$ (°C)	$T_h CO_2$ (°C)
1	−57.3	+8.2(L)
2	−56.8	+25.4(L)
3	−57	+21(L)
4	−57.4	+28.3(L)
5	−56.9	−3(L)
6	−56.7	−2(L)
7	−56.8	+7(L)
8	−56.9	+11(L)
9	−56.7	+26.3(L)
10	−56.7	−4(L)
11	−56.7	+1.7(L)
12	−56.6	+5(L)
13	−56.8	+9.3(L)
14	−56.8	+11(L)
15	−56.8	+12(L)
16	−57.1	+9.2(L)
17	−56.6	+16.6(L)
18	−56.6	+12.7(L)
19	−57	+5(L)
20	−60	+25(L)
21	−56.8	+28.2(L)
22	−56.6	+14(L)
23	−56.9	+15.8(L)
24	−57.1	+9(L)
25	−56.5	+5.6(L)
26	−57.1	+7(L)
27	−56.7	+12.8(L)
28	−56.6	+24(L)
29	−56.6	+21.9(L)
30	−56.8	+6(L)
31	−57.2	+14.6(L)
32	−56.6	+8.9(L)
33	−56.9	+26(L)

phase proportions and bulk properties as shown in (Fig. 9c). As a result the isochores, temperature of homogenization and state of homogenization will be different for each inclusion of that FIA.

From the results of fluid inclusion studies of WGF, the following inferences have been outlined and used for detailed discussion:

i. Three types of primary inclusions have been observed; Type-I: H_2O-CO_2 inclusions, Type-II: CO_2 inclusions and Type-III: Aqueous inclusions. The co-existence of Type-I and Type-II primary inclusions in a single quartz grain is very common.

ii. The phase proportions at room temperature in Type-I (H_2O : CO_2) and Type-III (liquid to vapour) inclusions range from 90 : 10 to 10 : 90 and 80 : 20 to 50 : 50, respectively (table). The range of total homogenization temperature (Th TOT) is very broad i.e. 194°C to 300°C for Type-I inclusions and 189°C to 282°C for Type-III inclusions. The Type-I inclusions homogenizes into both liquid and vapour state (table).

iii. The fluid involved in the mineralization of gold in WGF was H_2O-CO_2 dominant low saline (calculated average value of 8 wt % NaCl equivalents) with minor amount of other gases like N_2 and CH_4 as inferred from microthermometric analysis.

iv. The T_h TOT v/s salinity plot shows (Fig. 10) that there is a considerable variation of T_h TOT within a narrow range of salinity. This indicates the fluid immiscibility as reported in other areas such as Piaba gold deposit, São Luís cratonic fragment of Brazil and Xincheng deposit, Jiaodong Peninsula, China (de Freitas and Klein, 2013 and Wang et al., 2014).

Type-III primary fluid inclusions

S.No.	L : V at room temperature	T_h TOT (°C)	T_{FM} Ice (°C)	T_m Ice (°C)	Salinity Wt % NaCl eq
1.	80 : 20	205(L)	−20	−5	7.8
2.	80 : 20	248(L)	−39	−1.2	1.9
3.	70 : 30	282(L)	−29	−5	7.8
4.	50 : 50	251(L)	−29	−5	7.8
5.	80 : 20	189(L)	−21	−3	4.8
6.	70 : 30	243(L)	*	*	*

*—Not observed/Not calculated.
S.No—Serial Number.
T_h TOT—Temperature of total homogenization.
(L)—Homogenization into liquid state.
(V)—Homogenization into vapour state.
$T_h CO_2$—Temperature of homogenization of CO_2.
$T_m CO_2$—Temperature of first melting of CO_2.
T_m CL—Temperature of melting of clathrate.
T_{FM} Ice—Temperature of first melting of ice.
T_m Ice—Temperature of final melting of ice.
L : V—Liquid to vapour ratio.

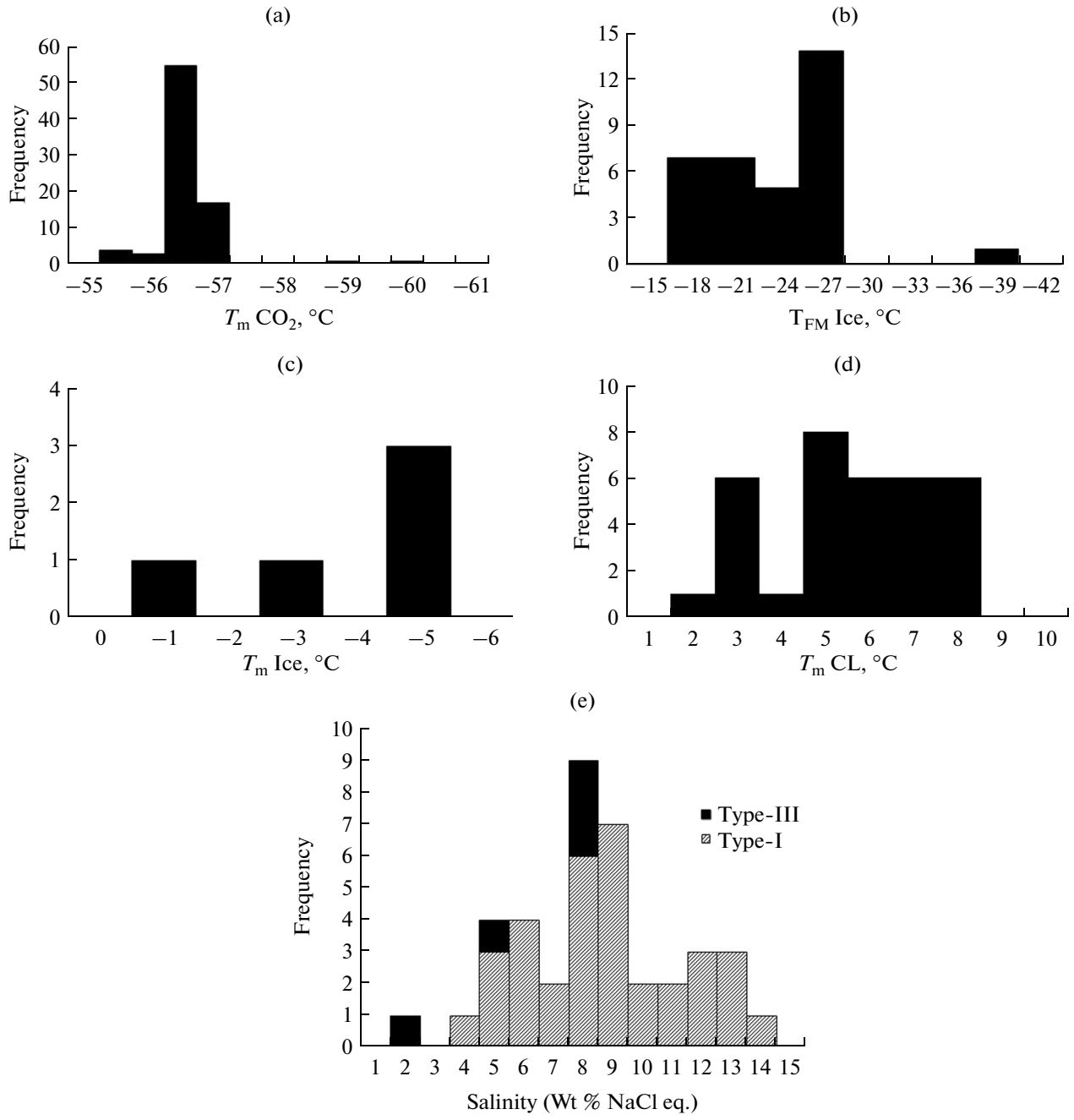

Fig. 6. Histograms of different parameters of primary inclusions obtained during freezing. (a) T_m CO_2 v/s frequency, (b) T_{FM} Ice v/s frequency, (c) T_m Ice v/s frequency, (d) T_m CL v/s frequency (e) Salinity v/s frequency.

On the basis of the above inferences and comparing with the concept of heterogeneous entrapment of fluid inclusions given by Diamond (2003), we consider that gold bearing homogeneous fluid became heterogeneous due to phase separation (fluid immiscibility) in WGF. Due to the heterogeneous entrapment of aqueous carbonic fluid, different kinds of primary fluid inclusions such as aqueous (Type-III), carbonic (Type-II) and aqueous-carbonic (Type-I) with different phase proportion were trapped (point i, ii and iii as mentioned in the inferences and Fig. 11). In addition to this, the broad range of total homogenization temperature, different state of homogenization (liquid and vapour) observed during thermometric runs (point ii as mentioned in the inferences and Fig. 8) and coexistence of Type-I and Type-II primary inclusions

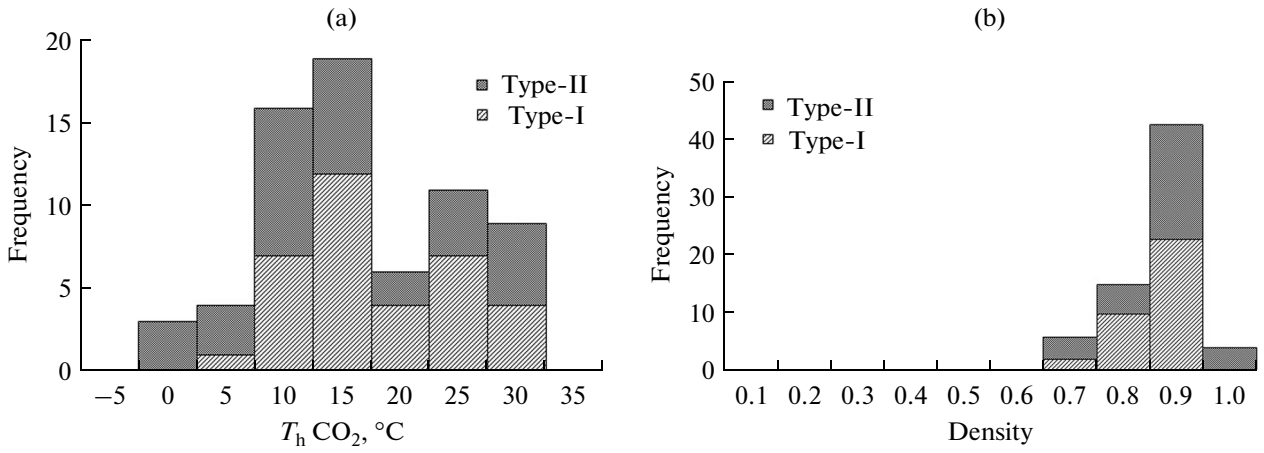

Fig. 7. Histograms of Th CO_2 v/s frequency (a) and Density of CO_2 v/s frequency (b).

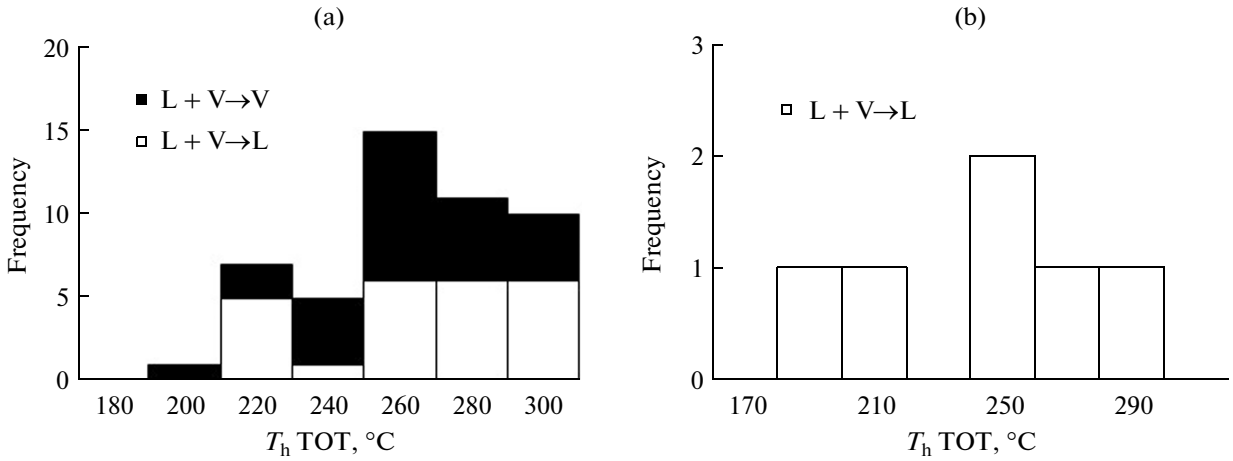

Fig. 8. Histograms of T_h TOT of Type-I inclusions v/s frequency (a) and T_h TOT of Type-III inclusions v/s frequency (b).

(point i as mentioned in the references and Fig. 4) are the important outcome of the current fluid inclusion studies on WGF samples. All these evidences support phase separation of original homogeneous ore forming fluid and consequent heterogeneous entrapment of aqueous carbonic gold bearing fluid in WGF. The results of studies by Caulibaly (2008), Yao et al. (2001) and Klemd (1998) related to lode gold deposits also indicated phase separation of ore forming fluid resulting in gold deposition.

Estimation of P-T conditions of Fluid Entrapment

The principal methods described by Shepherd et al. (1985) to estimate fluid pressure at the time of trapping are (i) the vapour pressure of the fluid at temperature of total homogenization, (ii) fluid isochores used in conjuction with independent geothermometers, (iii) intersecting isochores for coeval fluid and (iv) dissolution of daughter minerals (halite). The co-existance of Type-I and Type-II inclusions in the samples during the present work allowed us to use the intersecting isochores method. Isochores of Type-I and Type-II inclusions were plotted using Bowers and Helgeson (1985) and Holloway (1981)'s equations of state, respectively. P-T diagrams were constructed for three suitable cases of co-existance of Type-I and Type-II (Fig. 12). The temperature and pressure values of the intersection points are: 328°C/2.41 kbar (IP-1), 289°C/1.93 kbar (IP-2), 253°C/1.49 kbar (IP-3),

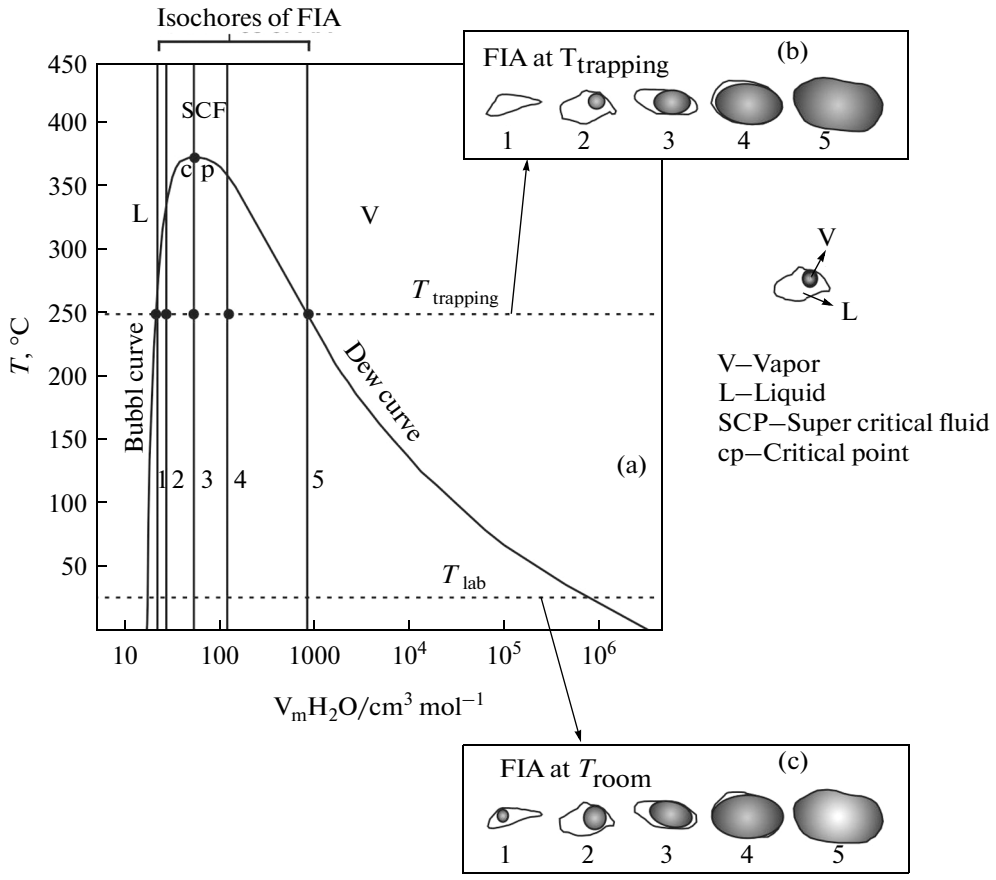

Fig. 9. Illustration of heterogeneous entrapment of a fluid inclusion assemblage (Diamond, 2003).

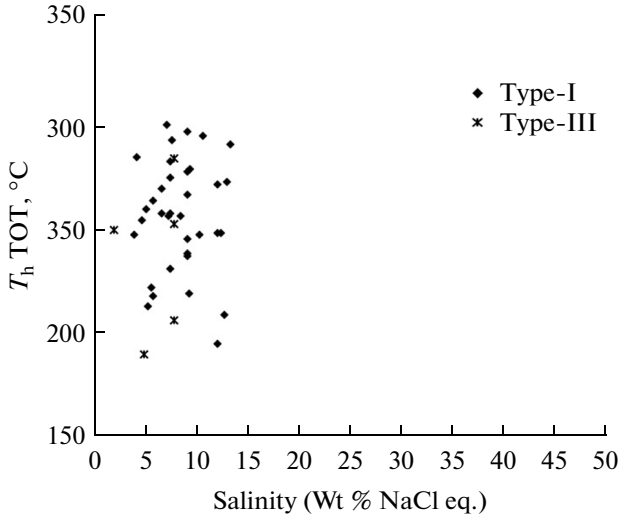

Fig. 10. T_h TOT v/s salinity plot of Type-I and Type-III inclusions.

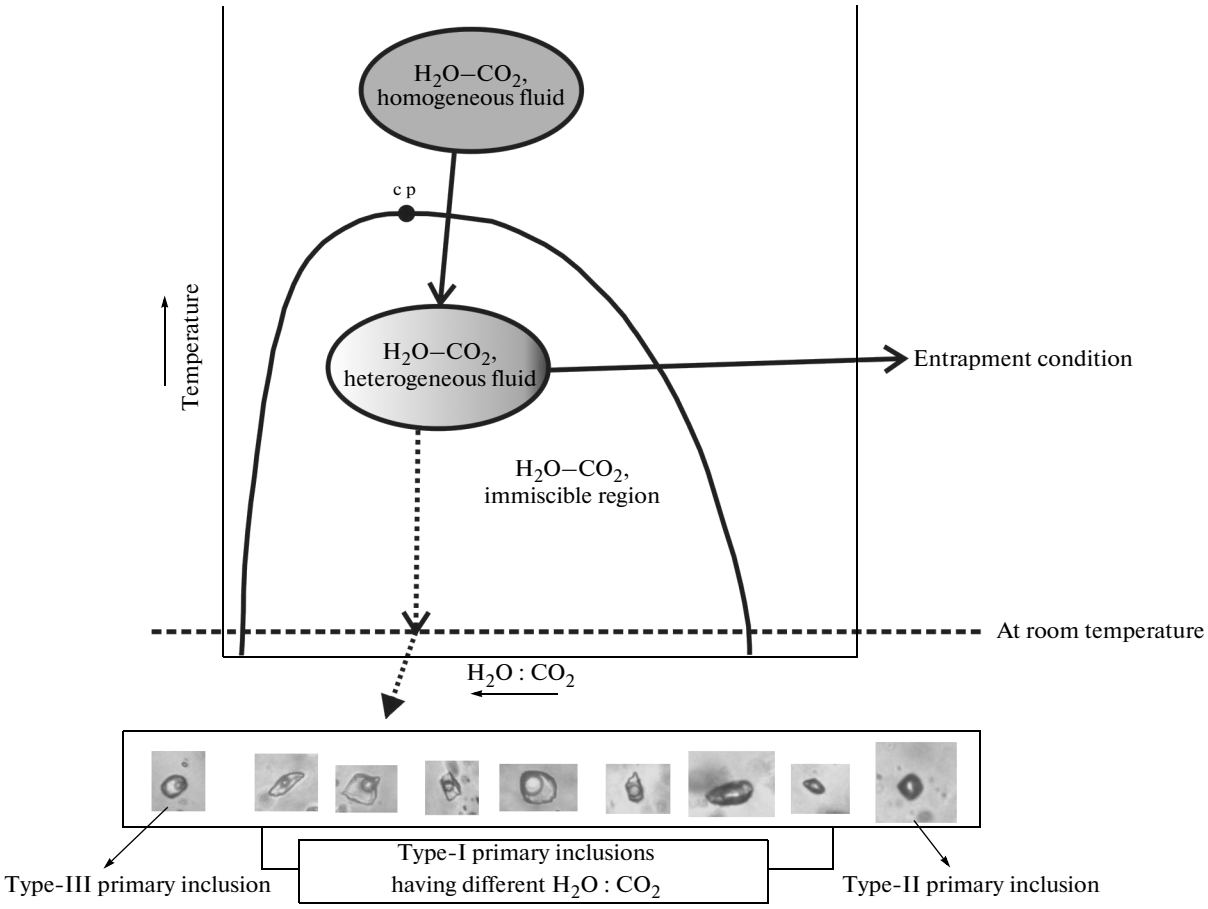

Fig. 11. Schematic diagram depicting the heterogeneous entrapment of original aqueous carbonic homogeneous fluid in WGF. Different kinds of primary inclusions (Type-I, Type-II and Type-III) have been shown at the bottom of the diagram. At room temperature the Type-III and Type-I inclusions appear bi-phase but were distinguished during microthermometric analysis (see section 5.1).

241°C/1.34 kbar (IP-4) and 237°C/1.42 kbar (IP-5). These estimated temperature and pressure values have been considered as P-T conditions of trapping of fluid inclusions in the auriferous quartz veins.

CONCLUSION

Our study indicates entrapment of immiscible fluids (i.e. heterogeneous entrapment) in inclusions present in auriferous quartz veins of WGF. The original homogeneous fluid in WGF was low saline $H_2O–CO_2$. The fluid was subjected to immiscibility (or phase separation) within temperature and pressure range of 240 to 330°C and 1.4 to 2.4 kbar. Gold along with other constituents could have precipitated in response to phase separation of the ore fluid. The phase separation of original homogeneous gold bearing ore fluid could be due to drop of pressure and temperature as it entered the fractures developed during the late phase of Neoproterozoic (Pan-African) deformation event.

ACKNOWLEDGMENTS

The Department of Science and Technology (DST), Government of India is acknowledged for providing a Heating-Freezing stage with Nikon Microscope as a part of Sponsored Research Project to Dr. R. Krishanmurthi, Professor, Department of Earth Sciences, Indian Institute of Technology Roorkee. The authors wish to thank Dr. Rajesh Sharma, Scientist of Wadia Institute of Himalayan Geology, Dehradun and Prof. A.K Sen, Department of Earth Sciences, IIT Roorkee for their help to improve the manuscript. Research Scholar Ms. Manju Narayanan is also acknowledged for her help during the course of this work. The authors thank Dr. V. Ravikant and

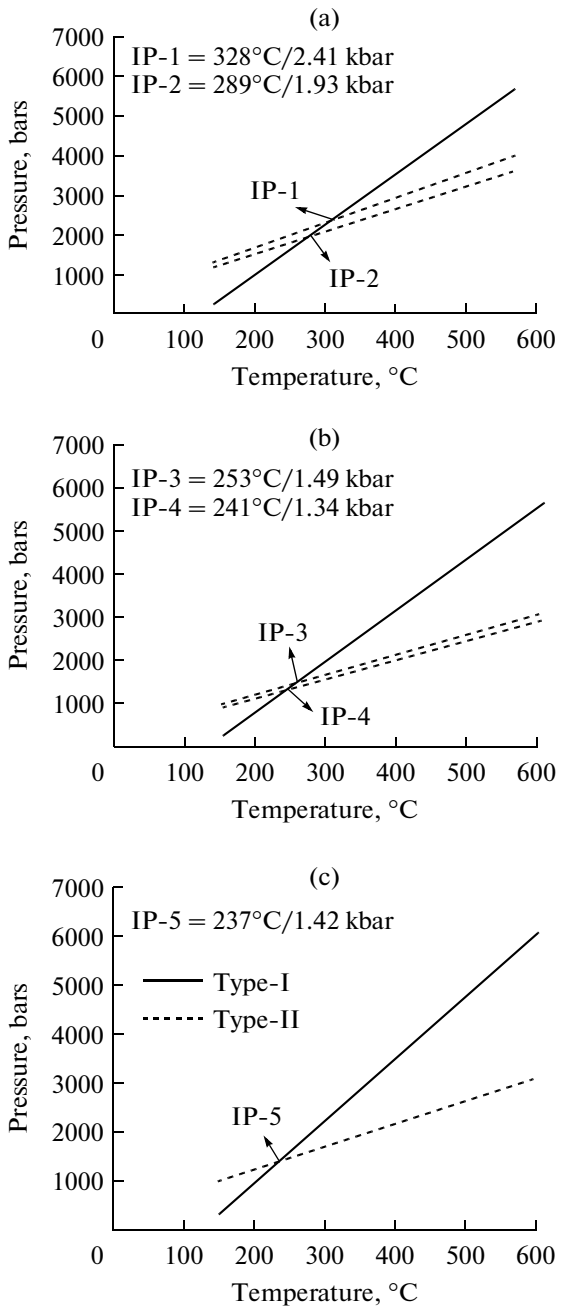

Fig. 12. Estimation of Pressure-Temperature conditions of fluid entrapment related to gold mineralization by intersecting isochores method using isochores of coexisting Type-I and Type-II inclusions.

Dr. K.L. Pruseth for lively discussion related to gold mineralization in WGF. The anonymous reviewer is deeply acknowledged for his/her comments to improve the quality of the manuscript.

REFERENCES

Benning, L.G. and Seward, T.M., *Hydrosulphide complexing of Au (I) in hydrothermal solutions from 150–400°C and 500–1500 bar, Geochim. Cosmochim. Acta,* 1996, vol. 60, pp. 1849–1871.

Binu Lal, S.S., Sawaki, T., Wada, H. and Santosh, M., Ore fluids associated with the Wynad gold mineralization, Southern India: Evidences from fluid inclusion microthermometry and gas analysis, *Asian J. Earth Sci.*, 2003, vol. 22, pp. 171–187.

Bowers, T.S. and Helgeson, H.C., FORTRAN programs for generating fluid inclusion isochores and fugacity coefficients for the system H_2O–CO_2–NaCl at high pressures and temperatures, *Comp. Geosci.*, 1985, vol. 1, pp. 203–213.

Brown, P.E., FLINCOR, A microcomputer program for reduction and investigation of fluid inclusion data, *Am. Mineral.*, 1989, vol. 74, pp. 1209–1221.

Chetty, T.R.K. and Rao, B., Behaviour of stretching lineations in the Salem-Attur Shear belt, Southern Granulite Terrain, south India, *Geol. Soc. India*, 1998, vol. 52, pp. 443–448.

Chetty, T.R.K., Fitzsimons, I., Brown, L., Dimri, V.P., and Santosh, M., Crustal structure and tectonic evolution of the Southern Granulite Terrain, India: Introduction, *Gondwana Res.,* 2006, vol. 10, pp. 3–5.

Chetty, T.R.K. and Santosh, M., Proterozoic orogens in southern Peninsular India: contiguities and complexities, *Asian J. Earth Sci.*, 2013, vol. 78, pp. 39–53.

Christopher, J.Y. and Vanderhor, F., Archaean lode-gold deposits, *J. Austral. Geol. Geophys.*, 1998, vol. 17, pp. 253–258.

Coulibaly, Y., Boiron, M.C., Cathelineau, M., and Kouamelan, A.N., Fluid immiscibility and gold deposition in the Birimian quartz veins of the Angovia deposit (Yaoure, Ivory Coast), *J. Afr. Earth Sci.,* 2008, vol. 50, pp. 234–254.

Diamond, L.W., Systematics of H_2O inclusions, in *Fluid Inclusions: Analysis and Interpretation*, Samson, I.M., Anderson, A.J., Marshall, D.D., Eds., *Mineral. Ass. Canada, 2003, Short Course*, 2003, vol. 32, pp. 55–79.

de Freitas, S.C. and Klein, E.L., The mineralizing fluid in the Piaba gold deposit, Sao Luis cratonic fragment (NW-Maranhao, Brazil) based on fluid inclusion studies in quartz veins, *Brazilian J. Geol.,* 2013, vol. 43, no. 1. Pp. 70–84.

Fyfe, W.S. and Kerrich, R., Gold: natural concentration processes, in *Gold '82: The Geology, Geochemistry and Genesis of Gold Deposits, Geol. Soc. Zimbabwe, Sp. Publ.,* 1982, No. 1, pp. 99–126.

Groves, D.I., The crustal continuum model for late-Archaean lode-gold deposits of the Yilgarn Block, Western Australia, *Miner. Deposita*, 1993, vol. 28, pp. 366–374.

Groves, D.I., Goldfarb, R.J., Gebre-Mariam, M., Hagemann, S.G., and Robert, F., Orogenic gold deposits: a proposed classification in the context of their crustal distribution and relationship to other gold deposit types, *Ore Geol. Rev.*, 1998, vol. 13, pp. 7–27.

Ho, S.E., Groves, D.I., and Phillips, G.N., Fluid inclusions as indicators of the nature and source of the ore fluids and ore depositional conditions for Archaean lode gold deposits of the Yilgarn Block, Western Australia, *Trans. Geol. Soc. S. Afr.*, 1985, vol. 88, pp. 149–158.

Holloway, J.R., Volumes and compositions of supercritical fluids, in *Fluid Inclusions: Petrologic Applications*, Hollister, L.S., and Crawford, M.L., Eds., *Mineral. Ass. Canada Short Course Handbook*, 1981, vol. 6, pp. 13–38.

King, W., Preliminary note on the gold fields of southeast Wynad, Madras, *Rec. Geol. Soc. India*, 1878, vol. 8, no. 2.

Klemd, R., High CO_2 content of fluid inclusions in gold mineralization in the Ashanti belt, Ghana: a new category of ore forming fluids? A comment, *Miner. Deposita*, 1998, vol. 33, pp. 317–319.

Krishnamurthi, R., What we do know about the genesis of gold mineralization in the Southern Granulite Terrain of Indian Peninsula, *J. Ind. Geol. Congress*, 2013, vol. 18, pp. 47–55.

Mikucki, E.J., Hydrothermal transport and depositional processes in Archean lode gold systems: a review, *Ore Geol. Rev.*, 1998, vol. 13, pp. 307–321.

Misra, K.C., *Understanding Mineral Deposits*, New York: Kluwer Academic Publishers, 2000.

Pruseth, K.L., Ravikant, V., Varghese, S., and Krisnamurthi, R., Mantle-derived carbonate fluid alteration and gold mineralization in Southen Granulite Terrain, Wynad, India, in *Dyke Swarms: Keys for Geodynamic Interpretation*, 2011, pp. 125–139.

Radhakrishna, B.P. and Curtis, L.C., Gold in India, *Sp. Publ. Geol. Soc. India*, 1999, pp. 200-209.

Ridley, J., Mikucki, E.J., and Groves, D.I., Archean lode-gold deposits: fluid flow and chemical evolution in vertically extensive hydrothermal systems, *Ore Geol. Rev.*, 1996, vol. 10, pp. 307–321.

Roedder, E., *Fluid Inclusions, Mineral. Soc. Am., Rev. Mineral.*, 1984, vol. 12.

Santosh, M. and Sajeev, K., Anticlockwise evolution of ultrahigh temperature granulites within continental collisional zones in southern India, *Lithos*, 2006, vol. 92, pp. 447–464.

Santosh, M., Xiao, W.J., Tsunogae, T., Chetty, T.R.K., and Yellappa, T., The Neoproterozoic subduction complex in southern India: SIMS zircon U–Pb ages and implications for Gondwana assembly, *Precambrian Res.*, 2012, vol. 192, pp. 190–208.

Seward, T.M., The transport and deposition of gold in hydrothermal systems, in *Gold '82: The Geology, Geochemistry and Genesis of Gold Deposits,* Foster, R.P., Ed., Rotterdam: A.A. Balkema, 1984, pp. 165–182.

Seward, T.M., Thio complexes of gold in hydrothermal ore solutions, *Geochim. Cosmochim. Acta*, 1973, vol. 37, pp. 379–399.

Shepherd, T.J., Rankin, A.H., and Alderton, D.H.M., *A Practical Guide To Fluid Inclusion Studies*, London: Blackie and Son, 1985.

Soman, K., *Geology of Kerala*, Bangalore: Geol. Soc. India, 2002.

Wang, Z.L., Yang, L.Q., Guo, L.N., Marsh, E., Wang, J.P., Liu, Y., Zhang, C., Li, R.H., Zhang, L., Zheng, X.L., and Zhao, R.X., Fluid immiscibility and gold deposition in the Xincheng deposit, Jiaodong Peninsula, China: a fluid inclusion study, *Ore Geol. Rev.*, 2015, vol. 65, pp. 701–717. http://dx.doi.org/10.1016/j.oregeorev.2014.06.006

Williams-Jones, A.E., Bowell, R.J., and Migdisov, A.A., Gold in solution, *Elements*, 2009, vol. 5, pp. 281–287.

Yao, Y., Murphy, P.J., and Robb, L.J., Fluid characteristics of granitoid hosted gold deposits in the birimian terrane of Ghana: a fluid inclusions microthermometric and Raman spectroscopic study, *Econ. Geol.*, 2001, vol. 96, pp. 1611–1643.

Zhang, L., Chen, H., Chen, Y., Qin, Y., Liu, C., Zheng, Y., and Jansen, N.H., Geology and fluid evolution of the Wangfeng orogenic-type gold deposit, Western Tian Shan, China, *Ore Geol. Rev.*, 2012, vol. 49, pp. 85–95.